

Direct evidence for the effect of lattice distortions in the transport properties of perovskite-type manganite films

R. P. Sharma, G. C. Xiong, C. Kwon, R. Ramesh, R. L. Greene, and T. Venkatesan

Center for Superconductivity Research, Department of Physics, University of Maryland, College Park, Maryland 20742

(Received 11 June 1996)

We report ion channeling investigations in crystalline colossal magnetoresistance films of $\text{Nd}_{0.7}\text{Sr}_{0.3}\text{MnO}_3$, $\text{Pr}_{0.7}\text{Ba}_{0.3}\text{MnO}_3$, and $\text{La}_{0.7}\text{Ba}_{0.3}\text{MnO}_3$. The measured full width at half maximum of the channeling angular scans exhibit a dramatic increase with decreasing temperature which is larger than expected from a simple Debye model. The temperature range where such a change is observed overlaps with the peak magnetoresistance regions in the three cases. The observed effect is an order of magnitude larger than previously found by volumetric measurements and seems to provide a direct evidence for a dynamic Jahn-Teller distortion. [S0163-1829(96)06638-6]

Recent observations¹⁻³ of a colossal magnetoresistance (CMR) effect in the doped manganese oxide films $R_{1-x}M_x\text{MnO}_3$ ($R=\text{La, Nd, Pr}$ and $M=\text{Sr, Ca, Ba}$) has revived interest in these materials. They have potential for applications in magnetic storage technology⁴ in addition to other possible applications. A prominent feature of these materials is a large maximum in the resistivity⁵ near the ferromagnetic transition temperature (T_c). The resistivity is dramatically decreased when an external magnetic field is applied leading to a very large (colossal) magnetoresistance values. The transport properties seem to be controlled by the motion of an e_g electron from a Mn^{3+} to a Mn^{4+} via the intervening oxygen. The localized Mn spin from the electron in the t_{2g} orbitals ($s=\frac{3}{2}$) plays an important role in this charge transport and alignment of the adjacent spins promotes transport. This has been qualitatively understood on the basis of a Zener double exchange (ZDE) model.⁶⁻⁹ Recent theoretical calculations¹⁰ showed that the large resistivities measured in these materials, significantly beyond the Mott limit, could not be explained by the ZDE model alone and an additional charge localization mechanism is needed. A dynamic Jahn-Teller distortion was proposed for this purpose.¹¹ For LaMnO_3 , which exhibits a cubic to tetragonal phase transition at about 750 K, Kanamori¹² deduced that the primary lattice distortion is a tetragonal distortion of the oxygen octahedra surrounding the Mn sites driven by a Jahn-Teller effect of the d orbitals. Millis¹³ has built upon Kanamori's model, including explicitly the ionic displacements at the manganese and oxygen sites, and has shown that the structural phase transition is driven to lower temperature with doping at the rare-earth sites, vanishing at the compositions studied in this paper. The message of their work is that in manganites with a strong electron phonon coupling and a strong propensity for a Jahn-Teller distortion, the transport properties and lattice distortions are intimately coupled.¹⁴ It is conjectured that the $\text{Mn}^{3+}-\text{O}^{2-}-\text{Mn}^{4+}$ bond angle plays a critical role in controlling the electronic transport, where deviations from 180° increases the resistance by lowering the overlap of the highly directional electronic orbitals of the oxygen and manganese atoms. A phase transition from a crystallographically distorted paramagnetic state with hopping-type conductivity, to an ordered ferromagnetic state will be accompanied by a dramatic reduction in resis-

tivity and a bond angle change. Changes in the bond angle will be equivalent to a static or dynamic distortion of the lattice (particularly when the hopping charge travels with the distortion as in a polaron model), which will result in a spatial displacement of an atom from a linear string of atoms of the same species in the crystal. The current understanding is that one would expect to see very little change in the spatial arrangement of the rare earth (A' site) and divalent metallic atoms (A site), while the manganese and the oxygen atoms would be expected to show dramatic temperature dependent static and dynamic distortions.

In this paper we report a study of ion channeling in the manganites as a function of temperature. This technique¹⁵ provides a direct real space probe of very small, of the order of 1 picometer (pm), displacements of atoms from their regular lattice sites, such as caused by structural distortions or lattice vibrations. For example, a $\text{Mn}^{3+}-\text{O}^{2-}-\text{Mn}^{4+}$ bond angle distortion of one degree would result in an effective static distortion of the lattice of the order of 3 pm. Energetic ions, incident along a major crystallographic direction, undergo a series of correlated, gentle, small-angle collisions and are steered by the atomic rows and planes of a single crystal or epitaxial film and thus get channeled. The channeling of incident ions among the atomic rows or between the planes of the crystal causes a one to two orders of magnitude reduction in a small impact parameter event such as Rutherford backscattering. The full width at half maximum (FWHM) of the rocking angle of incidence for channeling is functionally dependent on the incident ion energy, the atomic numbers of projectile and target, the interatomic spacings and most importantly for the present study, any displacements (static or vibrational) of the atoms from their regular lattice sites.

Our investigations were made in three doped manganite films, $\text{Nd}_{0.7}\text{Sr}_{0.3}\text{MnO}_3$ (NSMO), $\text{Pr}_{0.7}\text{Ba}_{0.3}\text{MnO}_3$ (PBMO), and $\text{La}_{0.7}\text{Ba}_{0.3}\text{MnO}_3$ (LBMO) with Curie temperatures, T_c , ranging 70–320 K. Direct evidence of lattice distortion was obtained in all the three cases. The distortion occurs near T_c and disappears as the temperature is lowered below the peak resistivity (T_p). T_p and T_c appear to be essentially the same in well-annealed films, although an accurate determination of T_c by low field susceptibility or neutron scattering has not been done for the films reported here.

The doped manganese oxide films were grown on $\langle 100 \rangle$ LaAlO_3 single-crystal substrates by pulsed laser deposition using targets of stoichiometric composition. The thickness of the films was about 150 nm. The as-grown films had nearly perfect epitaxial crystalline structure (i.e., ion channeling minimum yield of $\sim 3\%$). A standard four-probe method was used to measure the dc resistance of the samples. Under the present deposition conditions, substrate temperature around 700 °C and oxygen pressure of 200 to 300 mTorr, the T_p values in PBMO, NSMO, and LBMO films were at 70, 170, and 320 K, respectively. The magnetoresistance versus temperature measurements were performed in a superconducting magnet, with the applied magnetic field parallel to the film surface and to the current direction. The decrease in resistance at T_p exceeded two orders of magnitude in a magnetic field of 8 T for all the samples.

Ion channeling measurements have been carried out using a very well collimated beam (0.5 mm diameter and $<0.01^\circ$ divergence) of 1.5 MeV He ions obtained from a 1.7 MV tandem accelerator (NEC Pelletron). The sample was mounted with a thermally conducting paste on a precision four axis goniometer having an angular resolution of 0.01° . The target holder was thermally insulated from the goniometer and could be cooled down to 37 K via a flexible copper braid attached to a closed cycle refrigeration system. The effective pressure of condensable gases was reduced to a negligible level at the target surface by cryogenic shielding. The sample temperature was varied by a small 25 W heater, and could be maintained within ± 2 K at any desired temperature between 40 and 400 K.

The 1.5 MeV He⁺ beam was incident on the sample and the backscattered particles were detected in annular surface barrier detector of 300 mm² active area with a 4 mm diameter central hole and mounted along the beam axis at a distance of 7 cm from the target. This arrangement gave a Rutherford back scattering (RBS) signal with good statistics at a nominal dose of incident He ions, thus minimizing the radiation damage effects. The RBS spectrum obtained from a NSMO film is shown in Fig. 1. The RBS signals from Nd, Sr, and Mn are indicated in this figure and they overlap to a small extent with the background signal of La from the substrate. The film thickness was estimated to be 150 nm by a computer fitting program, where the thickness is iteratively adjusted until the theoretical curve matched the experimental plot. The accuracy is about 10%. For the channeling investigations, the single crystalline film axis $\langle 100 \rangle$ was first aligned parallel to the incident 1.5 MeV He⁺ beam direction. The channeling angular scans were made about this axis with the RBS gate including the signals from Nd, Sr, and Mn. This gate also contained a small background from La present in the substrate. Because the film is on top, the incident particle is required to traverse the film thickness twice before reaching the detector and thus the substrate element contribution is pushed to lower energies.

Two such scans taken at 50 and 175 K are shown in Fig. 2. The large reduction in counts to $<5\%$ of the random yield when the $\langle 100 \rangle$ axis of the specimen is aligned with the incident beam direction, demonstrates a high quality single crystalline film. The FWHM of the channeling angular scans made at eight different temperatures for the NSMO specimen is plotted in Fig. 3. A clear enhanced variation in FWHM is

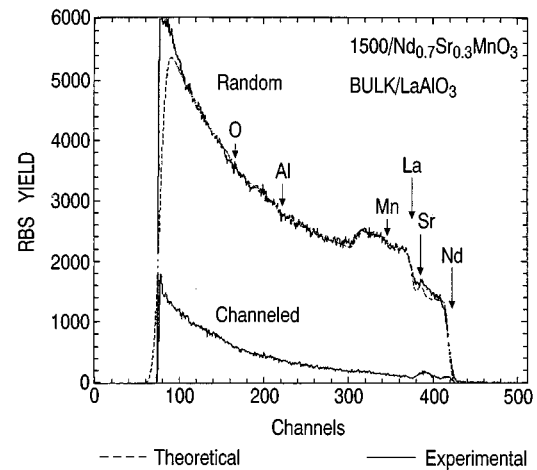


FIG. 1. The RBS spectrum of $\text{Nd}_{0.7}\text{Sr}_{0.3}\text{MnO}_3$ (NSMO) taken with 1.5 MeV He⁺ ions as a scattering range of 170° . The Nd and Sr edges are clearly seen while the Mn signals are mixed with those from Sr. The theoretical plot is shown by dotted line. Estimated thickness of the film is 150 nm. Also shown is the channeling spectrum.

seen as the temperature of the specimen is lowered through T_p . The FWHM of the channeling angular scan is directly related to small atomic displacements (thermal or static) from their regular lattice sites and normal to the channeling direction. In general, when the temperature of a solid is decreased there is a reduction in the thermal vibrational amplitude and accordingly an enhancement in the FWHM of the channeling angular scan. From the measured values of the FWHM, given in Fig. 3, the magnitude of the atomic displacement u is extracted using the continuum model¹⁶ for channeling, with corrections based upon the Monte Carlo computer simulation of Barrett¹⁷ and using average atomic numbers and lattice spacings. These u values for NSMO as a function of temperature are shown in Fig. 4(a). A larger change in the u values is seen in the vicinity of T_p . In order to show this variation clearly its derivative (du/dT) calculated by computer as a function of temperature is shown in Fig. 4(b), along with the resistance versus temperature plot

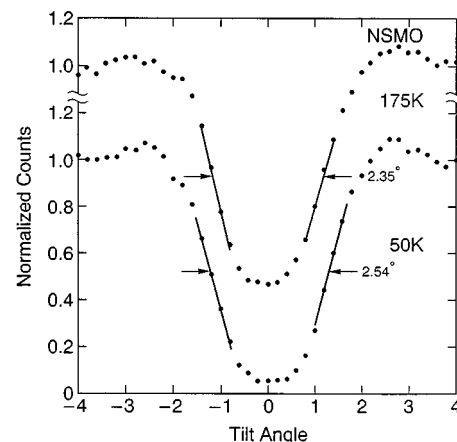


FIG. 2. The ion channeling angular scans (θ vs T) of NSMO single crystalline film taken at temperatures 50 and 175 K, respectively, are plotted one above the other, showing clearly the change in the FWHM.

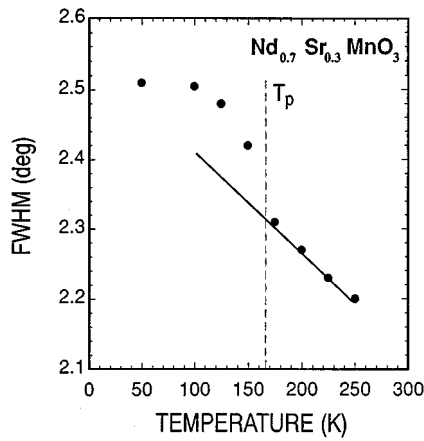


FIG. 3. A plot of the FWHM of channeling angular scans made in the NSMO film versus temperature. Note the large change in the value of FWHM in temperature interval 100 to 175 K.

of the same specimen. The rapid variation in u in the region of the resistance maxima is very clear.

Similar channeling measurements were made in PBMO and LBMO films. In the PBMO film the maximum in resistance is around 70 K while that in LBMO is close to room temperature. As in NSMO, the channeling angular scans taken with a PBMO film show an anomaly in the FWHM around T_p . A plot of $d\theta/dT$ vs T is shown in Fig. 5 along with the resistivity. A similar behavior is found in LBMO around the T_p of 320 K.

From the ferromagnetic resonance line width measurements, it appears that there is magnetic inhomogeneity in these films and therefore T_C may not be sharp and accordingly the variation in FWHM of the channeling angular scans is spread over different temperature ranges in the three samples mentioned above.

The smooth Debye-like behavior, i.e., a decrease in the thermal vibrational amplitude with decreasing temperature, is observed in all the three cases described above. However, there is an abrupt large decrease in the u value or increase in the FWHM in the vicinity of T_p as shown in Figs. 3, 4, and 5. This enhanced variation is unlikely to be caused by any abrupt thermal vibrational change, but is most likely related to structural distortions in the sample. The increase of the FWHM with reduction in temperature implies an increase in the crystallographic order. The present data yields a value of

1.0 to 2.0 pm for this displacement.

The current understanding of the zero-field transport behavior of these manganites is still in a state of evolution. These materials exhibit a paramagnetic semiconducting behavior above T_p and a metallic ferromagnetic phase below. Millis *et al.* proposed a model to explain this behavior involving a structural distortion due to a strong electron-phonon coupling arising from a Jahn-Teller splitting of the Mn^{3+} ions¹¹ coupled with a ZDE model. According to this model a phase transition from a crystallographically distorted state (paramagnetic semiconductor) with hopping-type conductivity to a more ordered ferromagnetic state (metallic conductor) occurs with a reduction in temperature. The role of the Jahn-Teller distortion is to essentially localize the carriers and the removal of the distortion, either by a reduction in temperature or by the application of an external field, causes a significant reduction in the resistivity. The precise nature of the distortion affecting the transport properties will require further studies but based on the present observations it is clear that distortions are playing an important role in the transport properties of these manganites.

In an earlier work the ion channeling investigations in antiferromagnetically ordered nickel chromite¹⁸ have provided indication of cooperative Jahn-Teller phase transition. In $NiCr_2O_4$, there is a well-defined cubic to tetragonal phase transition around 310 K, which has been interpreted to be a typical cooperative Jahn-Teller transformation. The present systems are different, being paramagnetic semiconductors above T_C , there is less likelihood of any cooperative Jahn-Teller effect. In any case the existence of cooperative effect could have been revealed by any number of other measurements such as neutron diffraction etc., while this is not the case. In the present system the distortions seems likely to be random, causing uncorrelated displacements of the Mn ions.

If we accept the idea of bond angle distortion for the $Mn^{3+}-O^{2-}-Mn^{4+}$, a static distortion of ~ 2 pm corresponds to a change in the bond angle of the order of 0.6° . Our results clearly show (Fig. 3) that once the film reaches the ferromagnetic state, there is no further change in the bond angle distortion in the system. Of the cations, one expects the maximum effect from the Mn sites while oxygen effects are not measured in the current experimental scheme. Since the backscattering counts are collected from the rare earth, divalent metal and as well as some contribution from the substrate, one measures a lower limit to the possible observable

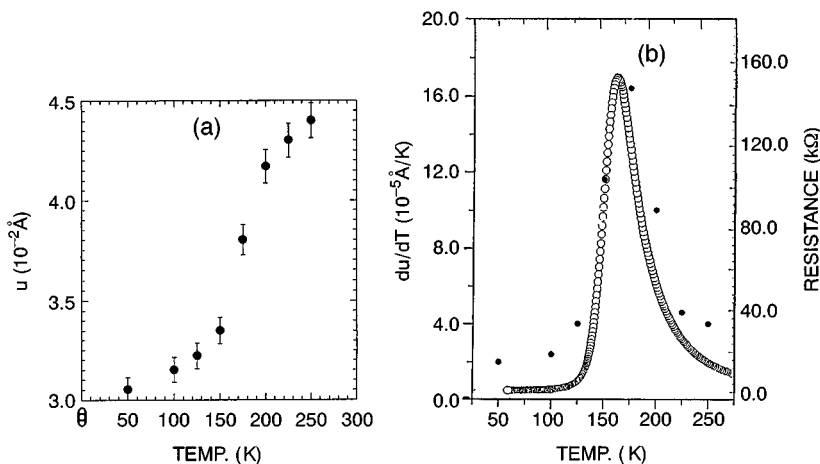


FIG. 4. (a) A plot of the atomic displacement u versus temperature for NSMO film, as obtained from the FWHM's given in Fig. 3(b). The du/dT vs T is shown by solid squares. Superimposed on it is the variation of resistance with temperature.

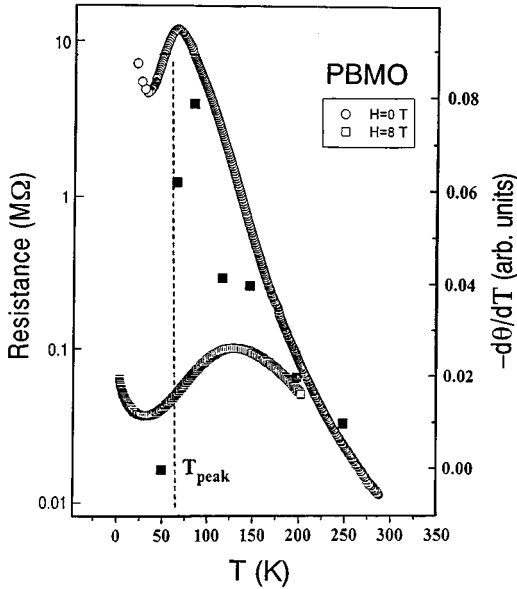


FIG. 5. The variation of the FWHM of channeling angular scans made in PBMO is shown by plotting $d\theta/dt$ vs T (solid squares). Superimposed on it is R vs T in PBMO. The two orders of magnitude drop in resistance in 8 T magnetic field is also shown.

distortion change. Surprisingly, the distortions measured from only the rare earth and the divalent metal sites is finite though one would expect most of the action to occur at the Mn and O site. In LBMO sample where the contribution from the La and Ba could be separated from that of Mn, it is seen that the reduction in distortion across T_C for these two elements is about half of the value where the Mn contribution is included. The distortion of the $\text{Mn}^{3+}\text{-O}^{2-}\text{-Mn}^{4+}$ bond, both in terms of the location of the oxygen atom with respect to the Mn^{3+} and the Mn^{4+} ion, as well as the bond angle, essentially destroys the center of symmetry of the system. Therefore one would expect a distortion of the A, A' site as well, and our observed results seem reasonable.

The channeling measurement does not distinguish between static and dynamic distortions. However, from volumetric measurements, in addition to the reduction due to thermal contraction, an abrupt decrease at T_p has been measured.¹⁹ The maximum change seen is $\sim 0.1\%$ which translates into a linear distortion of only 0.03% . Similarly, Ibarra *et al.*²⁰ report a large magnetovolume effect in Y doped LCMO where a similar lattice contraction of $\sim 0.04\%$ is seen in zero and applied magnetic field. In comparison, the distortion seen by ion channeling is more than an order of magnitude larger ($\sim 0.25\text{--}0.5\%$). This can only be explained if the distortion is dynamic and hence does not show up in volumetric measurements, much like a Debye-Waller type of atomic displacement. Based on this argument one can speculate that the observed large change in the lattice distortion with temperature may be a dynamic Jahn-Teller effect as had been proposed by Millis *et al.*¹¹

One can speculate on the origin of the dynamic Jahn-Teller distortion. Due to the electron phonon coupling, the oxygen octahedra surrounding the Mn ions is deformed. This deformation affects the cation-anion-cation ($\text{Mn}^{3+}\text{-O}^{2-}\text{-Mn}^{4+}$) bond angle in addition to a nonequivalence of cation-anion distances for the Mn^{3+} and Mn^{4+} ions.¹⁴ Deviations

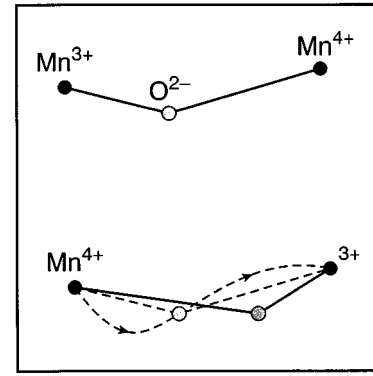


FIG. 6. Schematic of possible dynamic distortion in manganite films (NSMO, PMBO, and LBMO). The changes in $\text{Mn}^{3+}\text{-O}^{2-}\text{-Mn}^{4+}$ bond angle and the cation anion distance caused by distortion are shown in the upper part of the figure. During the process of double exchange, the bond length variation alternates between the two Mn and O ions as shown in the lower part of the figure.

from the cubic symmetry due to the Jahn-Teller interaction of Mn^{3+} ions as mentioned above seems to change the equilibrium bond angle by about 0.6° as estimated from our measured $\sim 1\text{--}2$ pm displacement. As shown in Fig. 6 the bond length between Mn^{3+} and O^{2-} is assumed to be smaller than that between O^{2-} and Mn^{4+} . During the process of double exchange these bond length variations may alternate between the two Mn and O ions. Thus as the transition temperature T_C is approached from above there is likely to be a structural instability in the material causing a dynamic incoherent displacement of atoms from their regular lattice sites. However, below the transition temperature the degeneracy of the ground state of Mn^{3+} ions is removed, because of the ferromagnetic field and the material tends towards an ordered state. Evidence for static and/or dynamic Jahn-Teller distortions of MnO_6 octahedra in perovskite-type manganites have also been found in recent²¹ neutron diffraction experiments. Theoretically the problem has been treated by Millis *et al.*¹¹ and also by Roder *et al.*²² by taking into account both dynamic Jahn-Teller and double exchange effects.

In conclusion, a quantitative measure of a possible dynamic Jahn-Teller distortion has been obtained in different manganite films as the films are cooled through the ferromagnetic transition. The distortions show a clear correlation with the transport properties. As the films go from a paramagnetic semiconductor to a ferromagnetic metal, the measured distortion ($\sim 1\text{--}2$ pm) decreases and reaches a steady state below T_C . The distortions are measured at both the B (Mn) and to a much lesser extent at the A (rare earth), A' (Ba, Ca, Sr, etc.) sites, indicating the absence of a center of symmetry due to these distortions. Experiments in which the thin film samples are prepared on a low Z substrate where the various individual peaks can be separated would enable us to measure the contribution from each site separately. However, the current data unambiguously demonstrates the role of a dynamical structural distortion and its correlation with the zero-field transport properties of the manganites.

We would like to acknowledge helpful discussions with S. M. Bhagat and S. Das Sarma. This work was performed under NSF Grant No. DMR 9510475.

- ¹R. von Helmholt, J. Wecker, B. Holzapfel, L. Schulz, and K. Samwer, *Phys. Rev. Lett.* **71**, 2331 (1993).
- ²S. Jin, T. H. Tiefel, M. McCromack, R. A. Fastnacht, R. Ramesh, and L. H. Chen, *Science* **264**, 413 (1994).
- ³H. L. Ju, C. Kwon, Qi Li, R. L. Greene, and T. Venkatesan, *Appl. Phys. Lett.* **65**, 2108 (1994).
- ⁴K. Derbyshire and E. Korczynski, *Solid State Technol.* **38-9**, 57 (1995).
- ⁵G. C. Xiong, Q. Li, H. L. Ju, S. N. Mao, L. Senapati, X. X. Xi, R. L. Greene, and T. Venkatesan, *Appl. Phys. Lett.* **66**, 1427 (1993).
- ⁶P. Zener, *Phys. Rev.* **82**, 403 (1951).
- ⁷P. W. Anderson and H. Hasegawa, *Phys. Rev.* **100**, 675 (1955).
- ⁸P. G. deGennes, *Phys. Rev.* **100**, 564 (1955).
- ⁹K. Kubo and N. Ohata, *J. Phys. Soc. Jpn.* **33**, 21 (1972).
- ¹⁰A. J. Millis, P. B. Littlewood, and B. I. Shraiman, *Phys. Rev. Lett.* **74**, 5144 (1995).
- ¹¹A. J. Millis, B. I. Shraiman, and R. Mueller, *Phys. Rev. Lett.* **77**, 175 (1996).
- ¹²J. Kanamori, *J. Phys. Chem. Solids* **10**, 87 (1959).
- ¹³A. J. Millis (unpublished).
- ¹⁴V. A. Bokov, N. A. Grigoryan, M. F. Bryzhina, and V. V. Tikhonov, *Phys. Status Solidi* **28**, 835 (1968).
- ¹⁵D. S. Gemmell, *Rev. Mod. Phys.* **46**, 129 (1974).
- ¹⁶J. Lindhard, *K. Dan. Vidensk. Selsk. Mat. Fys. Medd.* **34**, No. 14 (1965).
- ¹⁷J. H. Barrett, *Phys. Rev. B* **3**, 1527 (1971).
- ¹⁸D. Kollewe and W. M. Gibson, *Phys. Lett.* **65A**, 253 (1978).
- ¹⁹P. G. Radaelli, D. E. Cox, M. Mrezio, and S.-W. Cheong (unpublished).
- ²⁰M. R. Ibarra, P. A. Algarabel, C. Marquina, J. Blasco, and J. Garcia, *Phys. Rev. Lett.* **75**, 3541 (1995).
- ²¹P. G. Radaelli, M. Marezio, H. Y. Hwang, S-W. Cheong, and B. Batlogg (unpublished).
- ²²H. Roder, Jun Zang, and A. R. Bishop, *Phys. Rev. Lett.* **76**, 1356 (1996).